A Ray Tracing Algorithm Using the Discrete Prolate Spheroidal Subspace

Mingming Gan[1], Francesco Mani[2], Florian Kaltenberger[3], Claude Oestges[4], Thomas Zemen[1]
[1]FTW Forschungszentrum Telekommunikation Wien, Vienna, Austria
[2]COMELEC Department, Telecom ParisTech, France
[3]Mobile Communications Department, Eurecom, Sophia-Antipolis, France
[4]ICTEAM, Université catholique de Louvain, Louvain-la-Neuve, Belgium

***Abstract*—Ray tracing (RT) is an accurate propagation prediction tool that has been widely used to simulate channel characteristics in indoor environments. To date, the developed RT tool includes not only specular reflection, penetration through dielectric blocks and diffraction, but also diffuse scattering mechanisms. The accuracy, provided by a detailed modeling of the environment, comes at the cost of a high computational complexity, which directly scales with the number of propagation paths considered. We are interested in simulating the radio propagation conditions for a mobile terminal, communicating in a frame based communication system indoors with several fixed nodes. This communication shall be used to obtain the position of the mobile terminal in indoor scenario. Therefore, the correlated temporal and spatial evolution of the channel impulse response is of utmost concern. In this paper, we propose a method to significantly reduce the computational complexity of RT by using a projection of all propagation paths on a subspace spanned by two-dimensional discrete prolate spheroidal (DPS) sequences. With this method the computational complexity can be reduced by more than one order of magnitude for indoor scenarios. The accuracy of our low-complexity DPS subspace based RT algorithm is verified by numeric simulations.**

***Keywords*—ray tracing (RT), indoor, time-variant, low-complexity, discrete prolate spheroidal (DPS) sequences.**

I. Introduction

RT used in the present work is three-dimensional, which allows to accurately calculate the wireless propagation conditions for indoor environments. It relies on a geometric optical approach, which evaluates all propagation paths as they interact with the environment. RT considers line-of-sight (LOS) propagation, as well as reflection, penetration and diffraction components [1].

Furthermore, diffuse scattering components prove to be an important factor in determining time and angle dispersion of radio signals in indoor environments [2]. The inclusion of all these propagation mechanisms allows an accurate modeling of the temporal and spatial evolution of the channels impulse response, which is the major focus of the modeling effort described in this paper.

It is known that diffuse scattering components can be assumed spatially uncorrelated in indoor environments for different transmitter (Tx) and receiver (Rx) coordinates separated by many multiple wavelength [3]–[5]. However, the correlation of diffuse scattering components needs to be considered in the time-variant case where the Rx is moving only a short distance. As it is known for frame based communication systems, the moving distance of the Rx during the transmission of a single frame is typically smaller than one wavelength. This paper focuses on the development of a novel RT algorithm for such a scenario with low-computational complexity.

Moreover, for the test and development of indoor localization algorithms accurate indoor channel modeling is extremely important. It is well known that non-line-of-sight (NLOS) propagation paths introduce large errors for determining the mobile position. The reason is that localization algorithms often heavily rely on the information extracted from the LOS path such as the received signal strength (RSS), time of arrival (TOA), or time difference of arrival (TDOA) [6]. The diffuse scattering components take up a fairly large number of the NLOS propagation paths in an indoor scenario. Therefore, the diffuse scattering components are significant for indoor mobile localization and tracking algorithms. Recently, new localization methods have been proposed that can take advantage of multipath propagation [7], [8].

In this paper, we develop a RT algorithm for a time-variant indoor scenario, where (i) all objects and the Tx are static, and (ii) the Rx is moving with a constant speed along a linear trajectory. The main contribution of this paper are the following:

- For the simulation of a mobile terminal, the correlated evolution of diffuse scattering components within a short distance is considered. We extend the diffuse scattering algorithm for rough surfaces developed in [2], [4] to involve temporally correlated realizations for the single bounce scattering case.
- For indoor environments the large number of diffuse propagation paths causes a high computational complexity for standard RT algorithms. It is known for band-limited fading processes that a projection on a subspace spanned by two-dimensional discrete prolate spheroidal (DPS) sequences [9] allows for a substantial complexity reduction of geometry based stochastic channel models [10], [11]. We apply this concept to RT and develop a RT algorithm with a strongly reduced numerical complexity.

The paper is organized as follows: Section II describes the implemented RT channel model. The low-complexity approximation algorithms to significantly reduce the simulation

complexity is introduced in Section III. Section IV presents the simulation environment and evaluates numerically the accuracy of the proposed RT algorithm. Finally, we conclude in Section V.

II. RT Channel Model

RT includes three major wave propagation mechanisms: (i) LOS, (ii) specular components as well as (iii) diffuse scattering. It relies on the calculation of all propagation paths connecting the Tx and the Rx location for a given propagation mechanism. The RT channel model enables the calculation of the electric field in amplitude, phase and polarization at the mobile terminal position [12].

For a static Tx and a mobile Rx the channel impulse response becomes time-variant. More precisely, the channel is dependent on the Rx's position $\boldsymbol{x}$, whose relation with time t can be given as $\boldsymbol{x}(t) = \boldsymbol{x}_0 + \boldsymbol{v}_{\mathrm{Rx}} t$, where $\boldsymbol{x}_0$ is the initial position of the Rx when it starts moving, and $\boldsymbol{v}_{\mathrm{Rx}}$ is the velocity vector of the Rx.

Therefore, we use $H(f, \boldsymbol{x}(t))$ to express the time-variant channel frequency response in this paper. In wireless communications, the signal arriving at the Rx usually consists of several multipath components, each of which is arising from the interaction of the transmitted signal with the surrounding environment. Thus, the time-variant frequency response of RT $H_{\mathrm{RT}}(f, \boldsymbol{x}(t))$ can be seen as a superposition of all propagation paths' contributions, which can be calculated as

$$H_{\mathrm{RT}}(f, \boldsymbol{x}(t)) = \sum_{n=1}^{N} \eta_n(\boldsymbol{x}(t)) e^{-j2\pi f \tau_n(\boldsymbol{x}(t))}, \tag{1}$$

where n is the propagation path index, $\eta_n(\boldsymbol{x}(t))$ is the complex-valued weighting coefficient of the $n-$th path, $\tau_n(\boldsymbol{x}(t))$ is the delay, and N is the total number of paths. Both $\eta_n(\boldsymbol{x}(t))$ and $\tau_n(\boldsymbol{x}(t))$ depend on the Rx's position $\boldsymbol{x}(t)$. Based on the sampling rate in time $1/T_{\mathrm{S}}$, the sampled position vector of the Rx can be expressed as $\boldsymbol{x}[m] = \boldsymbol{x}_0 + \boldsymbol{v}_{\mathrm{Rx}} T_{\mathrm{S}} m$, where $m \in \{0, \ldots, M-1\}$ denotes the discrete time index and M is the number of samples in the time domain, respectively. With the sampling rate in distance $\boldsymbol{x}_{\mathrm{S}} = \boldsymbol{v}_{\mathrm{Rx}} T_{\mathrm{S}}$ we can express the sampled time-variant frequency response as

$$H_{\mathrm{RT}}[q, m] = H_{\mathrm{RT}}(q f_{\mathrm{S}}, \boldsymbol{x}_0 + m\boldsymbol{x}_{\mathrm{S}}) = \sum_{n=1}^{N} \eta_n[m] e^{-j2\pi q \theta_n[m]}, \tag{2}$$

where $q \in \{-\lfloor \frac{Q}{2} \rfloor, \ldots, \lfloor \frac{Q}{2} \rfloor - 1\}$ is the discrete frequency index, $f_{\mathrm{S}} = B/Q$ denotes the width of a frequency bin, B denotes bandwidth, Q is the number of samples in the frequency domain, and $\theta_n[m] = \tau_n[m] f_{\mathrm{S}}$ is the normalized delay of the $n-$th path at time m.

A. Specular Components

The mentioned specular components refer to reflection, penetration and diffraction contributions. The geometrical relationships between the incident and the reflected/penetrated/diffracted rays are based on optical principle. We use the approximation that the path direction of a ray undergoing penetration is not modified by this interaction [4]. Complex dyadic coefficients for the reflection and penetration are obtained using Fresnel formulas [13], while the diffraction coefficient is calculated by the uniform theory of diffraction (UTD) [14]. The computation of the complex-valued weighting coefficient $\eta_n[m]$ of the $n-$th single specular contribution at time m is implemented as described in [4], [12], [15], [16].

B. Diffuse Scattering with Correlation in Space

A flat wave is scattered into multiple (random) directions due to interaction with a rough surface, which is opposed to specular reflection in a single direction on a smooth surface. We are extending the algorithm of [4] to allow for correlated diffuse scattering which is relevant to simulate short movement of the Rx $|\boldsymbol{x}[M-1] - \boldsymbol{x}_0| \leq \kappa\lambda$, where $\kappa \leq 1$, and λ is the wavelength. The diffuse scattering components can be assumed correlated in time/space for this short distance [17]. It should be mentioned that we set $\kappa = 1$ at first and the value of κ will be finally defined by the mean square error (MSE) threshold described in Section IV-B.

We define the Rx's moving distance $\kappa\lambda$ as one simulation set, then RT should redraw the diffuse scattering components independently for another set. In the following we present the extended diffuse scattering algorithm for RT that enables the calculation of correlated realizations in one simulation set:

- The rough surface is divided into multiple tiles. A diffuse scattering path is supposed to arise from the center of each tile. The size of each tile is evaluated by recursively dividing the surface until the far-field condition is fulfilled [4]:
$$r_\ell < \sqrt{\frac{d_\ell[0]\lambda}{2}}, \tag{3}$$
where ℓ is the surface tile index, r_ℓ is the size of the $\ell-$th surface tile and $d_\ell[0]$ is the distance between the center of the $\ell-$th surface tile and the Tx for the single bounce scattering case. Since the Tx is static, the tiling of the surface for the duration $m \in \{0, \ldots, M-1\}$ is fixed.
- A scattering pattern model [2] evaluating the amplitude of each diffuse scattering path is related to each surface. In this paper, a directive pattern model is used, which assumes that the scattering lobe is steered towards the direction of the specular reflection [2], [4]. The amplitude of a diffuse scattering path $|\eta_\ell[m]|$ at time m can be computed as:
$$|\eta_\ell[m]|^2 = |\eta_{\ell_0}[m]|^2 \cdot \Big(\frac{1 + \cos(\varphi_\ell[m])}{2}\Big)^{\alpha_{\mathrm{r}}}, \tag{4}$$
where $|\eta_{\ell_0}[m]|$ is the maximum amplitude related to the $\ell-$th scattering lobe, $\varphi_\ell[m]$ is the angle between the scattering wave and the reflection wave directions, and α_{r} is an integer defined as the width of the scattering lobe.
- The complex-valued scattered weighting coefficient can be written as
$$\eta_\ell[m] = |\eta_\ell[m]| e^{-j\phi_\ell} \tag{5}$$
where ϕ_ℓ is the random phase associated with the $\ell-$th diffuse scattering path with an uniform distribution in

$[0, 2\pi]$. The random phase ϕ_ℓ is chosen at $m = 0$ and kept fixed for the duration $m \in \{0, \ldots, M-1\}$.

III. Complexity Reduction

Indoor environments with diffuse scattering require the calculation of a high number of propagation paths for RT. Hence there is a strong need to reduce the complexity of RT in order to enable its application to time and frequency selective channels. A two step approach is used to achieve this goal.

A. First Step: Sum of Complex Exponentials (SoCE) Channel Model

The geometrical calculation of all propagation paths have a significant impact on the complexity of RT in time-variant indoor environment for a moving Rx. In the case of $\kappa \leq 1$, it is sufficient to perform RT at the starting position $\boldsymbol{x}_0$ of the Rx. For the remaining linear movement distance $\boldsymbol{x}[m] = \boldsymbol{x}_0 + m\boldsymbol{x}_\mathrm{S}$, during the transmission in the simulated time range $m \in \{0, \ldots, M-1\}$ and frequency range $f \in [f_\mathrm{c} - B/2, f_\mathrm{c} + B/2]$, the channel is assumed to be wide sense stationary. Therefore, we can utilize the SoCE channel model [11] to reduce the numerical complexity. The sampled time-variant frequency response can be expressed as

$$H_\mathrm{SoCE}[q, m] = \sum_{n=1}^{N} \eta_n[0] e^{-j2\pi q \theta_n[0]} e^{j2\pi m \nu_n[0]}. \tag{6}$$

where $\eta_n[0]$, $\theta_n[0]$ and $\nu_n[0] = \omega_n[0] T_\mathrm{S}$ are the complex-valued weighting coefficient, normalized delay and normalized Doppler shift of the $n-$th path at the Rx's position $\boldsymbol{x}_0$. The Doppler shift ω_n at the center frequency f_c is given as $\omega_n[0] = f_\mathrm{c}(|\boldsymbol{v}_\mathrm{Rx}| \cos(\phi_n[0]))/c_0$, where c_0 is the speed of light and $\phi_n[0]$ is the angle of arrival of the $n-$th path.

B. Second Step: DPS Subspace Channel Model

We exploit the band-limited property of the channel impulse response projecting each path $n \in \{1, \ldots, N\}$ on a subspace spanned by two-dimensional discrete prolate spheroidal (DPS) sequences [9]. To design the DPS subspace we need two key parameters:

- the maximum normalized Doppler shift $\nu_\mathrm{Dmax} = \omega_\mathrm{max} T_\mathrm{S}$, where ω_max is the maximum Doppler shift, and
- the maximum normalized delay $\theta_\mathrm{Dmax} = \tau_\mathrm{max} f_\mathrm{S}$, where τ_max is the maximum delay.

The band-limited region is defined by the Cartesian product $\mathcal{W} = W_t \times W_f = [-\nu_\mathrm{Dmax}, \nu_\mathrm{Dmax}] \times [0, \theta_\mathrm{Dmax}]$. It is our interest to compute the channel response for a certain number of time stamps and frequency bins. We denote this index set as $\mathcal{I} = I_t \times I_f = \{0, \ldots, M-1\} \times \{-\lfloor \frac{Q}{2} \rfloor, \ldots, \lfloor \frac{Q}{2} \rfloor - 1\}$.

The approximate two-dimensional DPS subspace representation $H_\mathrm{DPS}^{(D)}$ with the subspace dimension D, can be expressed as [10]

$$H_\mathrm{DPS}^{(D)}[q, m] \approx \boldsymbol{V} \tilde{\boldsymbol{\alpha}}, \tag{7}$$

where the two-dimensional DPS basis vectors are

$$\boldsymbol{V} = \boldsymbol{V}(\mathcal{W}, \mathcal{I}) = \boldsymbol{V}(W_t, I_t) \diamond \boldsymbol{V}(W_f, I_f). \tag{8}$$

The operator $\diamond$ is the Tracy-Singh product of column-wise partitioned matrices [18]. $\boldsymbol{V}(W_t, I_t)$ and $\boldsymbol{V}(W_f, I_f)$ have the essential subspace dimensions D_0 and D_1 in space/time and frequency, respectively. The approximated basis coefficients are represented as

$$\tilde{\boldsymbol{\alpha}} = \sum_{n=0}^{N-1} \eta_n[0] (\underbrace{(\boldsymbol{V}(W_t, I_t) \boldsymbol{\chi}_t(\nu_n))}_{\boldsymbol{\gamma}_n^t : \approx \tilde{\boldsymbol{\gamma}}_n^t(\nu_n; W_t, I_t)} \otimes \underbrace{(\boldsymbol{V}(W_f, I_f) \boldsymbol{\chi}_f(\theta_n))}_{\boldsymbol{\gamma}_n^f : \approx \tilde{\boldsymbol{\gamma}}_n^f(\theta_n; W_f, I_f)}), \tag{9}$$

where the complex exponential functions $\boldsymbol{\chi}_t(\nu_n)$ and $\boldsymbol{\chi}_f(\theta_n)$ are given as

$$\boldsymbol{\chi}_t(\nu_n) = [\vartheta_t^0, \vartheta_t^1, \ldots, \vartheta_t^{(M-1)}]^T, \tag{10}$$

and

$$\boldsymbol{\chi}_f(\theta_n) = [\vartheta_f^{(-\lfloor \frac{Q}{2} \rfloor)}, \vartheta_f^{(-\lfloor \frac{Q}{2} \rfloor + 1)}, \ldots, \vartheta_f^{(\lfloor \frac{Q}{2} \rfloor - 1)}]^T, \tag{11}$$

where $\vartheta_t = e^{j2\pi\nu_n[0]}$ and $\vartheta_f = e^{-j2\pi\theta_n[0]}$. $\tilde{\boldsymbol{\gamma}}_n^t(\nu_n; W_t, I_t)$ and $\tilde{\boldsymbol{\gamma}}_n^f(\theta_n; W_f, I_f)$ are the approximated projections of the complex exponential functions on the DPS basis vectors in time and frequency dimensions, which can be calculated by the scaled and shifted approximated DPS wave functions [10].

The computation time of the DPS subspace channel model needs to consider the simulation time T_RT of an initial RT result. The runtime of RT at each $m \in \{1, \ldots, M-1\}$ is almost the same as the runtime at $m = 0$, the approximated computation effort of the DPS subspace channel model can be given as

$$\frac{M T_\mathrm{RT}}{T_\mathrm{RT} + T_\mathrm{DPS}} < M, \tag{12}$$

where T_DPS is the runtime of the DPS algorithm without the computation of an initial RT result. The details about T_DPS are described in [10]. Therefore, the computational complexity reduction factor of the DPS method is bound by the number of time samples M.

IV. Simulation Procedure

RT depends on a full description of the scenario to be simulated. In order to show the performance of the proposed RT channel model, a time-variant indoor scenario is generated. The simulated indoor scenario is shown in Figure 1.

A. Simulation Configuration

The size of the scenario is about 13m × 24m × 4.5m. The materials sketched with cyan, yellow and red lines represent concrete, wood and brick walls, respectively. The input database also contains dielectric properties of the materials. The values of relative permittivity ε_r and the conductivity σ of the materials involved in the simulated scenario are presented in Table I. The transmitting and receiving antennas used for the simulation are dipole antennas with the length $\lambda/2$. The Rx antenna is linearly moving with a constant speed and along a constant direction.

We take into account LOS, reflection (up to the third order), single diffraction and single bounce scattering. Note that the penetration case is embedded into all other contributions. The visualization of some ray paths are also shown in Figure 1.

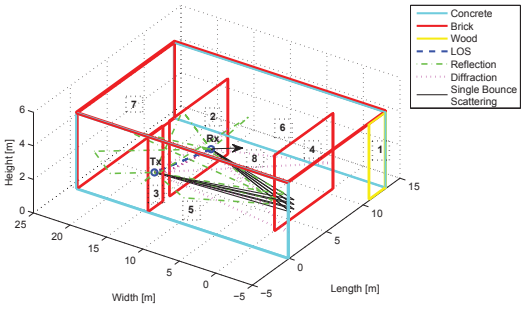

Fig. 1. Indoor time-variant scenario with a static Tx and a mobile Rx. Each block is indexed by a number.

TABLE I
DIELECTRIC PROPERTIES OF THE MATERIALS [5]

Materials	ε_r	σ [S/m]
Concrete	6	0.08
Wood	2.1	0.05
Brick	4	0.005

There are more than $N = 3.4 \times 10^3$ ray paths to be calculated at one time m. Firstly, we set $\kappa = 1$, hence the Rx moves one wavelength. Initial simulation parameters are summarized in Table II.

B. Numerical Results

The MSE between RT and the SoCE channel model can be calculated as (13) [1]

$$err(\boldsymbol{x}(t)) = \frac{\int |H_{\text{RT}}(f, \boldsymbol{x}(t)) - H_{\text{SoCE}}(f, \boldsymbol{x}(t))|^2 df}{\int |H_{\text{RT}}(f, \boldsymbol{x}(t))|^2 df}. \quad (13)$$

The associated result is shown in Figure 2. By setting the error threshold $err_{\text{thr}} = -20$dB, the corresponding moving distance of the Rx is $|\boldsymbol{x}_{\text{thr}}| = 0.25\lambda$, which is equivalent to 0.03m. Therefore, we finally define $\kappa = 0.25$. Furthermore, keeping $|\boldsymbol{x}_{\text{S}}|$ fixed, the number of time samples $M = 25$ for the remaining of this paper.

Within the threshold region, the Rx moving distance is finally clarified as one-quarter wavelength. The approximation errors among RT, SoCE and DPS subspace channel models, which can be calculated similarly to (13), are shown in Figure 3. It can be noticed that the maximum MSE of the low-complexity DPS subspace channel model is more than 40dB below the power of the SoCE channel response. Meanwhile

TABLE II
INITIAL SIMULATION PARAMETERS

Parameter	Value
Carrier frequency f_{c}	2.45 GHz
Bandwidth B	240 MHz
Rx velocity $\lvert\boldsymbol{v}_{\text{Rx}}\rvert$	3 km/h
Sampling rate in distance $\lvert\boldsymbol{x}_{\text{S}}\rvert$	0.0012 m
Number of time samples M	100
Width of frequency bin f_{S}	500 KHz
Number of frequency bin Q	480

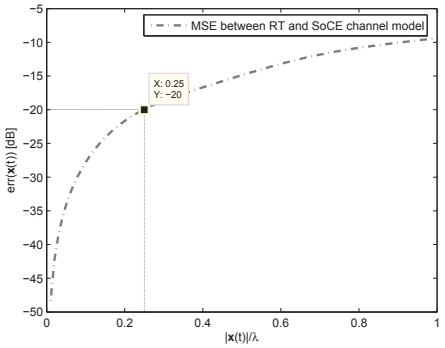

Fig. 2. MSE between RT and SoCE channel model. The moving distance of Rx is one wavelength. The error threshold is set as -20dB.

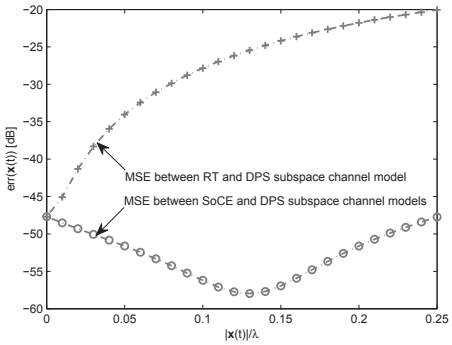

Fig. 3. MSE among RT, SoCE and DPS subspace channel models. The moving distance of Rx is one-quarter wavelength.

the MSE between RT and DPS subspace channel model is smaller than the error threshold err_{thr}.

The numerical complexity for the simulated channels is significantly reduced with a negligible approximation error. Considering the same time-variant indoor scenario, where the Rx moves about one-quarter wavelength within $M = 25$ time samples, the RT runs about 555.10s, while the DPS subspace channel model requires roughly 9.30s plus the simulation time of the initial RT result of 24.46s. Figure 4 presents the simulation time comparison between the RT and DPS subspace channel model within different number of blocks N_{b} in the indoor scenario. It is obvious that a scenario with more objects, modeled as rectangular blocks, leads to an increase in the number of propagation paths and the simulation time of RT. According to (12), the computational complexity reduction factor of the DPS method is bound by the number of time samples 25. When there are 4 and 8 blocks in the scenario, the complexity reduction factors achieved by the DPS subspace channel model are 2 and 16, respectively. The computational complexity reduction achieved by the DPS method increases with the number of propagation paths when the number of time samples M is fixed. It can be seen that the simulation time of the DPS method without the computation of an initial RT result does not change much with the increasing number of

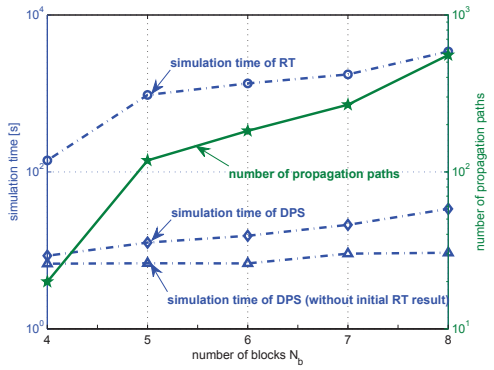

Fig. 4. Simulation time comparison according to different number of blocks in the scenario: RT and DPS. N_b is corresponding to the first indexed N_b blocks in Figure 1. Rx moves about one-quarter wavelength within $M = 25$ time samples.

TABLE III
DPS PARAMETERS

DPS Parameter	Value
Maximum norm. Doppler ν_{Dmax}	0.01
Subspace dimension D_0	4
Maximum norm. delay θ_{Dmax}	0.13
Subspace dimension D_1	131

propagation paths. The runtime comparison shown in Figure 4 also correlates nicely with exact result presented in [10]. The parameters of the DPS sequences with $N_\mathrm{b} = 8$ blocks in the scenario are summarized in Table III. It is evident that the subspace dimensions are much smaller than the number of propagation paths.

V. CONCLUSION

In this paper, we presented a low-complexity RT algorithm to reduce the computation time of RT in time-variant indoor environments. The temporal correlation of the diffuse scattering components was considered for a short moving distance of the Rx. In the first step, the SoCE channel model was applied to reduce the RT complexity. The accuracy of the SoCE channel model with respect to RT was verified using an error threshold. In order to further reduce the simulation time, the two-dimensional DPS subspace channel model was implemented to approximate the SoCE model. The computational complexity reduction factor of the proposed RT algorithm using the DPS subspace is bound by the number of time samples. Furthermore, the computational complexity reduction achieved by the DPS subspace channel model increases with the number of propagation paths when the number of time samples was fixed. In future work, we will address the accuracy validation for the low-complexity RT algorithm based on measurements.

ACKNOWLEDGMENT

This work was supported by the project NFN SISE (S10607) funded by the Austrian Science Fund (FWF). The Austrian Competence Center "FTW Forschungszentrum Telekommunikation Wien GmbH" is funded within the program COMET - Competence Centers for Excellent Technologies by BMVIT, BMWFJ, and the City of Vienna. The COMET program is managed by the FFG. It was also carried out in cooperation within the COST IC1004 Action. Claude Oestges is pleased to acknowledge the financial support of the Belgian Fonds de la Recherche Scientifique - FNRS (FRS-FNRS).

REFERENCES

[1] G. Tiberi, S. Bertini, W. Malik, A. Monorchio, D. Edwards, and G. Manara, "Analysis of realistic ultrawideband indoor communication channels by using an efficient ray-tracing based method," *Antennas and Propagation, IEEE Transactions on*, vol. 57, no. 3, pp. 777 – 785, Mar. 2009.

[2] V. Degli-Esposti, F. Fuschini, E. M. Vitucci, and G. Falciasecca, "Measurement and modelling of scattering from buildings," *Antennas and Propagation, IEEE Transactions on*, vol. 55, no. 1, pp. 143 – 153, Jan. 2007.

[3] F. Mani and C. Oestges, "Evaluation of diffuse scattering contribution for delay spread and crosspolarization ratio prediction in an indoor scenario," in *Antennas and Propagation (EuCAP), 2010 Proceedings of the Fourth European Conference on*, April 2010, pp. 1 – 4.

[4] F. Mani, F. Quitin, and C. Oestges, "Accuracy of depolarization and delay spread predictions using advanced ray-based modeling in indoor scenarios," *EURASIP Jounal in Wireless Commmunications and Networking*, vol. 2011, p. 11, 2011.

[5] ——, "Directional spreads of dense multipath components in indoor environments: Experimental validation of a ray-tracing approach," *Antennas and Propagation, IEEE Transactions on*, vol. 60, no. 7, pp. 3389 – 3396, July 2012.

[6] H. Chen, G. Wang, Z. Wang, H. So, and H. Poor, "Non-line-of-sight node localization based on semi-definite programming in wireless sensor networks," *Wireless Communications, IEEE Transactions on*, vol. 11, no. 1, pp. 108 – 116, Jan. 2012.

[7] T. Öktem and D. Slock, "Power delay doppler profile fingerprinting for mobile localization in NLOS," in *Personal Indoor and Mobile Radio Communications (PIMRC), 2010 IEEE 21st International Symposium on*, Sep. 2010, pp. 876 – 881.

[8] T. Callaghan, N. Czink, F. Mani, A. Paulraj, and G. Papanicolaou, "Correlation-based radio localization in an indoor environment," *EURASIP Journal in Wireless Commmunications and Networking*, 2011.

[9] D. Slepian, "Prolate spheroidal wave functions, fourier analysis, and uncertainty - V:the discrete case," *The Bell System Technical Journal*, vol. 57, no. 5, pp. 1371 – 1430, 1978.

[10] F. Kaltenberger, T. Zemen, and C. W. Ueberhuber, "Low-complexity geometry-based MIMO channel simulation," *EURASIP Jounal in Advanced Signal Processing*, vol. 2007, 2007.

[11] N. Czink, F. Kaltenberger, Y. Zhou, L. Bernado, T. Zemen, and X. Yin, "Low-complexity geometry-based modeling of diffuse scattering," in *Antennas and Propagation (EuCAP), 2010 Proceedings of the Fourth European Conference on*, April 2010, pp. 1 – 4.

[12] C. Oestges, B. Clerckx, L. Raynaud, and D. Vanhoenacker-Janvier, "Deterministic channel modeling and performance simulation of microcellular wide-band communication systems," *Vehicular Technology, IEEE Transactions on*, vol. 51, no. 6, pp. 1422 – 1430, Nov. 2002.

[13] S. U. Inan and S. A. Inan, *Electromagnetic Waves*. Prentice, 2000.

[14] R. Luebbers, "Finite conductivity uniform GTD versus knife edge diffraction in prediction of propagation path loss," *Antennas and Propagation, IEEE Transactions on*, vol. 32, no. 1, pp. 70 – 76, Jan. 1984.

[15] C. Oestges and Vanhoenacker-Janvier, "Experimental validation and system applications of ray-tracing model in built-up areas," *Electronics Letters*, vol. 36, no. 5, pp. 461 – 462, Mar. 2000.

[16] F. Mani and C. Oestges, "A ray based indoor propagation model including depolarizing penetration," in *Antennas and Propagation, 2009. EuCAP 2009. 3rd European Conference on*, Mar. 2009, pp. 3835 – 3838.

[17] J. Karedal, F. Tufvesson, N. Czink, A. Paier, C. Dumard, T. Zemen, C. Mecklenbrauker, and A. Molisch, "A geometry-based stochastic MIMO model for vehicle-to-vehicle communications," *Wireless Communications, IEEE Transactions on*, vol. 8, no. 7, pp. 3646 – 3657, July 2009.

[18] T. Zemen and A. Molisch, "Adaptive reduced-rank estimation of nonstationary time-variant channels using subspace selection," *Vehicular Technology, IEEE Transactions on*, vol. 61, no. 9, pp. 4042 – 4056, Nov. 2012.